LRP 605/98 May 1998

# Global Ideal MHD Stability of Plasmas with Toroidal, Helical and Vertical Field Coils

A. Ardelea, W.A. Cooper, L. Villard

Submitted for Publication to
Plasma Physics & Controlled Fusion

# Global ideal MHD stability of plasmas with toroidal, helical and vertical field coils

A. Ardelea, W. A. Cooper, L. Villard

April 28, 1998

Centre de Recherches en Physique des Plasmas (CRPP/EPFL), Association Euratom-Confédération Suisse, CH-1015 Lausanne, Switzerland

**Abstract**

A simple configuration that consists of a set of toroidal, helical and vertical field coils is used to calculate free boundary equilibria with nonzero plasma current and approximately helically symmetric plasma boundary shape. The amount of helical boundary deformation is controlled by the ratio of the current in the helical field coils to the current in the toroidal field coils. When this ratio is increased, the $(m, n) = (2, 1)$ external kink is stabilized at $\beta \simeq 1\%$ for inverse rotational transform profiles in the region $q < 2$ and an aspect ratio $A \simeq 10$.

# 1 Introduction

In tokamak machines a strong plasma current is indispensable for the plasma confinement and plays a significant role in plasma heating. It is known that this current may generate disruptions with dangerous consequences for the machine components. Stellarators can achieve plasma confinement without net plasma current and avoid thus disruptions but have other kinds of drawbacks. The absence of symmetry can adversely impact particle confinement and transport.The lack of ohmic heating requires auxiliary systems (rf waves or neutral beam injection) which increase the total cost of the machine and the complex three-dimensional (3D) structure of the magnetic field imposes strong accuracy conditions when manufacturing and assembling the coils.

During the last years some papers have appeared in the literature presenting new concepts for confinement devices. The terminology was enriched with terms like Spherical stellarators [1], stellamaks [2] or more general designations like tokamak-stellarator hybrids [3], [4]. Characteristic of these machines is the fact that they combine the standard coil system of a tokamak with a set of twisted or simple planar coils inclined vertically responsible for stellarator effects. The net toroidal plasma current is non zero and the machines based on these concepts should be able to operate in hybrid manner depending on how the two systems of coils are powered (a significant part of the rotational transform can be produced by the current flowing in the external coils). Until now the study of these concepts focused on issues like $B$ (magnetic field) properties, vacuum flux surface characteristics, bootstrap currents estimations and particle confinement analysis. A general study of the MHD stability of these configurations and in particular of the current-driven kink modes has not been yet considered.

In earlier studies [5] or in more recent ones [6], [7], a series of authors considered the effect of adding an external rotational transform on kink stability. The analysis were however limited to pressureless, straight plasma columns with uniform or non uniform $j$ toroidal plasma currents and most of them to the cases when $\iota_h$ (the external rotational transform) added to the system was constant. The results were expressed in the form of analytical conditions for the stability of a given $(m, n)$ mode generally with low $m$, $n$. It

was stated in [7] that a sufficient high external rotational transform can stabilize all ideal kink modes.

In the context of the development of the hybrid machine concepts, the study of the effects of external rotational transform on kink mode stability in realistic 3D configurations appears fully justified. In a previous work [8], the authors of the present paper studied the kink modes in three dimensional plasmas with prescribed (fixed) helical boundary deformation and non vanishing toroidal current; the external rotational transform resulted from the prescription of the boundary shape and the total $\iota$ was determined from the equilibrium computations. More precisely, $L = 2,\ 3$ configurations with single helicity and mixtures of both were considered and the stability was tested with respect to the $(m, n)$ external kink modes with $n = 1, 2, 3$ (toroidal mode number) and $m = n + 1$ (poloidal mode number). The equilibrium parameters like the amount of helical boundary deformation, the aspect ratio, the number of equilibrium field periods, the toroidal current density, $\beta$ and the pressure profiles were systematically varied in that investigation. Once these parameters were fixed, sequences of equilibria differing in the amount of helical boundary deformation and such that $1 \leq q \leq 2 - 2.5$ ($q$ is the inverse rotational transform), were calculated with the fixed boundary version of the VMEC [9] code. The ideal MHD stability analysis was performed with the TERPSICHORE [10] code. It was shown that increasing the helical boundary deformation leads to the stabilization of $(m, n)$ external kinks with $n = 1, 2, 3$, $m = n + 1$ at values of $\beta \simeq 1 - 2\%$. These modes are unstable in the circular tokamak at the same value of $\beta$. If $\delta$ is the amplitude of the Fourier components responsible for the helical shape of the boundary, then windows of stability $[\delta_{min}\ \ \delta_{max}]$ may exist depending strongly on the other equilibrium parameters. The present paper reconsiders the effect of the helical boundary deformation on kink mode stability but in the case where the numerical equilibria are calculated with a free boundary. The geometry of the external coils responsible for stellarator effects is taken into account; the ratio between the current in the external helical coils and the plasma current replaces the $\delta$ parameter and represents the fundamental input parameter in the investigation. The paper is divided as follows: section II and III explain how the equilibrium and stability calculations were performed, section IV presents some specific results

and section IV contains the summary and conclusion.

# 2 Equilibrium calculations

The calculations of the free boundary equilibria were performed in several steps. First, a system of coils producing a toroidal field (TF), a vertical field (VF) and a helical field (HF) is designed; the helical conductors are wound on a torus according to the winding law

$$v = \frac{1}{N_{per}}(\tilde{u} + \alpha sin(\tilde{u})) - \frac{l}{L}\frac{2\pi}{N_{per}} \qquad \tilde{u} = u + 2\pi\frac{l-1}{L} \tag{1}$$

with $u$ and $v$ the geometrical poloidal and toroidal angles of a particular coil segment, $N_{per}$ the number of field periods, $l = 1,..L$ an index specifying a particular coil and $\alpha$ the pitch modulation coefficient of the helical coils. The magnetic field $\vec{B}$ is determined from the Biot-Savart law and a field line tracing code is used to find the coil geometrical parameters and currents such as to obtain closed helical flux surfaces in vacuum. The field produced by these external currents is given then as input to the free-boundary version of the equilibrium code VMEC [11]. At finite $\beta$ and nonzero plasma current, the plasma cross section is distorted; the currents in the coils are adjusted until the plasma cross section recovers an approximate helical shape. Several types of coils systems (stellarator-, heliotron- and torsatron-like) were considered. We illustrate the results with the example of a L=2 stellarator-like configuration ($N_{per} = 4$) with 16 TF coils, two pairs of HF coils and one pair of VF coils. Sequences of equilibria were calculated with the following parameters

$$R_0 = 5.0\,[m] \;\; r_t = 1.8\,[m] \;\; r_h = 1.4\,[m] \;\; r_v = 7.0\,[m] \;\; z_v = \pm\, 2.1\,[m] \;\; \alpha = -0.150$$

$$I_t = -1.6 \times 10^5[A] \qquad\qquad I_v = 1. \times 10^4[A] \tag{2}$$

$$\beta = 1\% \text{ , parabolic pressure profile , } J'(s) \sim (1 - s^{20})^8$$

The subscripts $_t$, $_h$ and $_v$ refer to the TF, HF and VF coils respectively, $R_0$ is the major radius, $r$ and $z$ identify the distances of the coils from the major axis and the horizontal midplane reespectively, $I$ refers to the coil currents and $J'$ is the toroidal plasma current

density profile. $0 \leq s \leq 1$ is the radial variable proportional to the enclosed toroidal magnetic flux. The equilibria belonging to one particular sequence differ in the amount of HF coil current $I_h$. The coil system is illustrated in Fig.1 and the plasma cross sections for three values of $I_h$ are shown in Fig.2. For these calculations the plasma current was $J = 127\,kA$. If the conventional (tokamak) definition of normalized beta $\beta_N = \beta/I_N$ with $I_N = J\,[MA]/(a\,[m]\,B_0\,[T])$ where $a$ and $B_0$ are the averaged minor radius and the magnetic field intensity on the axis respectively, is used we obtain $\beta_N \sim 4 - 6$.

# 3 Stability analysis

The variational formulation of the linear ideal MHD stability of 3D plasmas on which TERPSICHORE is based is described in detail in [12]. The variational equation is written as:

$$\delta W_p + \delta W_v - \omega^2 \delta W_k = 0 \tag{3}$$

where $\delta W_p$, $\delta W_v$, $\delta W_k$ and $\omega^2$ represent the potential energy in the plasma, the magnetic energy in the vacuum region, the kinetic energy and the eigenvalue of the system. The perturbations have been assumed to evolve as $exp(i\omega t)$ and the system is unstable to MHD modes when $\omega^2 < 0$. The contribution of the vacuum to the potential energy is treated according to the pseudoplasma technique [13] which considers the vacuum region as a pressureless, shearless and massless pseudoplasma. The stability problem in vacuum is similar in form to that in the plasma [12].

In the TERPSICHORE code, the stability problem is formulated in Boozer coordinates [14]. The equilibrium is remapped to this coordinate system and the perturbation components are expressed in truncated Fourier series with respect to the angular variables $\theta$ and $\phi$. Let $(m_e, N_{per} n_e)$ and $(m_l, n_l)$ represent Fourier components in Boozer coordinates of the equilibrium and perturbation quantities respectively. The contribution to the plasma and vacuum potential energy of the coupling between any two perturbation components involves integrals of the type [12]

$$\int\int d\theta\, d\phi\; A_{m_e,n_e}(s)\; f_e(m_e\theta - N_{per} n_e \phi)\; f_1(m_{l1}\theta - n_{l1}\phi)\; f_2(m_{l2}\theta - n_{l2}\phi) \tag{4}$$

where $f_e$, $f_1$ and $f_2$ are *sin* or *cos* functions. The $A_{m_e,n_e}$ quantity represents the amplitude of the equilibrium component; it is a function of the radial flux coordinate $s$. The coupling between the two perturbation components $(m_{l1}, n_{l1})$ and $(m_{l2}, n_{l2})$ is nonzero if the following relations hold between the mode numbers [15], [16], [8] :

$$\begin{aligned} m_e &= m_{l1} \pm m_{l2} \\ n_e N_{per} &= n_{l1} \pm n_{l2} \end{aligned} \tag{5}$$

This means that a partial decoupling of the perturbation components occurs, depending on the values of the toroidal mode numbers; the perturbation toroidal mode numbers are distributed in families between which there are no interactions. Within this context, the expression $(m, n)$ mode means that the $(m, n)$ Fourier component of the perturbation (in Boozer coordinates) is dominant with respect to the other components.

If $N_{per} = 4$ and the mode studied is $(m, n) = (2, 1)$, then the contribution of the coupling $(m_e, N_{per}n_e) \times (2, 1) \times (m_l, n_l)$ to the potential energy is nonzero only if $n_l = 3$, 5, 7, 9, etc - c.f. Eq.(5). When the numerical study is carried in the parameter region corresponding to $1 \leq q(s) \leq 2$ which is the region where the (2,1) mode may be strongly destabilizing, then a particular attention should be given to those $(m_l, n_l)$ perturbation components which are resonant i.e. $m_l > n_l > n = 1$. Depending on the $q$ profile, these components can be destabilized and could lead a priori to significant couplings with $(2, 1)$. The contribution of a particular $(m_{l1}, n_{l1}) \times (m_{l2}, n_{l2})$ nonzero coupling to the potential energy - let us denote it by $W_p^{(m_{l1},n_{l1})\times(m_{l2},n_{l2})}$, is determined by the amplitude $A_{me,ne}$ of the $(m_e, N_{per}n_e)$ equilibrium coupling term. Typical $A_{me,ne}$ terms appearing in these couplings are $\sqrt{g}_{m_e,n_e}$ (the Jacobian), $|B^2|_{m_e,n_e}$ or combinations between the coefficients of the metric tensor [12]. It can be seen from Eq.(5) that if $N_{per} = 4$ the coupling between $(2, 1)$ and $(m_l, n_l)$ resonant components with $n_l = 3, 5$ requires $(m_e, N_{per}n_e)$ components with $n_e = 1$ and $m_e > 4$; the coupling with resonant $(m_l, n_l)$ having $n_l = 7, 9$ requires $n_e = 2$ and $m_e > 8$. Table 1 illustrates these combinations.

The numerical study performed in [8] has shown that a characteristic property of the equilibria with fixed helical boundaries is that those $A_{me,ne}$ amplitudes (in Boozer coordinates)

involved in couplings between $(m,n)$, $m=n+1$, $n=1,2,3$ and the resonant $(m_l,n_l)$ are negligible compared to the amplitudes of the dominant equilibrium components. This is true $\forall s$ (on each flux surface) for equilibrium quantities like $\sqrt{g}_{m_e,n_e}$ , $|B^2|_{me,ne}$ , etc ; it was checked for different types and amounts of helical boundary deformation, different number of periods $N_{per}$, and a multitude of equilibrium profiles (current density, pressure). Fig.3a illustrates this for a particular case i.e. a $L=2$ configuration with $N_{per}=4$: the $A_{me,ne}$ coupling $(2,1)$ to the resonant components $(m_l>n_l>1)$ are at least 3 orders of magnitude smaller than the dominant $A_{me,ne}$.

If the equilibrium is calculated with a free boundary and the currents in the coils - see Fig.1 - are adjusted such that the free boundary plasma has an approximate helical boundary shape - see Fig. 2, then the above mentioned property remains valid. Fig.3b shows $A_{me,ne}$ amplitudes for an equilibrium belonging to the sequence characterized by Eq.(2) and calculated for $I_h=110\,kA$. This equilibrium is situated between those corresponding to $I_h=100\ kA$ and $I_h=130\ kA$ for which the flux surface cross sections have been represented in Fig.2 (2nd and 3rd row). The consequence of this property is that, the numerical study of a mode like $(m,n)=(2,1)$ does not require taking into account the $(m_l,n_l)$, $m_l>n_l>1$ perturbation components (with $n_l$ and $n=1$ belonging to the same family). This conjecture was systematically checked: it was found that if the resonant $(m_l,n_l)$ are included in the calculations, then, the $W_p^{(m,n)\times(m_l,n_l)}$ contributions with $(m,n)=(2,1)$, $(1,1)$ and $m_l>n_l>1$, are negligible when compared to the dominant contributions to the potential energy. When one does not include the resonant $(m_l,n_l)$ components the numerical effort is reduced and it becomes easier to follow the evolution of the $(m,n)$ mode studied.

# 4 Results

Once an equilibrium sequence has been calculated by increasing $I_h$ uniformly, the main task of the stability analysis consists in the successive determination of the unstable eigenvalues $\omega^2$ starting with the most unstable $\omega^2_{min}$ and the identification of the perturbation components associated with them. This is done for every $I_h$. In the first step the calculations are performed excluding the resonant $(m_l,n_l)$, $m_l>n_l>1$ perturba-

tion components. At the beginning of the equilibrium sequence presented in Fig.4 i.e for $I_h = 60\ kA$ the $q$ profile is such that the $(2,1)$ component is already destabilized. The effect of increasing $I_h$ is to lower the inverse rotational transform. The $(2,1)$ component is strongly destabilized and becomes the dominant perturbation component - the $(2,1)$ mode. The most unstable eigenvalue $\omega^2_{min}(I_h)$ decreases until a minimum is attained, after which it starts increasing again; this is the stabilizing effect associated with an increasing (approximately) helical boundary deformation. Depending on the equilibrium parameters, a stability window $I_{stb} = [I_h^{min}, I_h^{max}]$ may appear in the sense that all $(m,1)$ components with $m > 1$ are stable and the $(1,1)$ component is not yet destabilized. Fig.4 (c) illustrates a stability window bounded by $I_h^{min} \simeq 100\ kA$ and $I_h^{max} \simeq 130\ kA$.

When the resonant perturbation components i.e. $(m_l, 3)$ with $m_l > 3$, $(m_l, 5)$, etc, are taken into account and the stability calculations are performed again for those equilibria in the stable window, then several unstable eigenvalues may appear for each $I_h \in I_{stb}$. Each of these eigenvalues is associated to one of the resonant $(m_l, n_l)$ modes (component with largest amplitude) and the most important contributions to the potential energy come from terms like $W_p^{(m_l,n_l)\times(m_{l'},n_{l'})}$ with $m_l > n_l > 1$ and $m_{l'} > n_{l'} > 1$. Table 2 illustrate these results for three selected equilibria from the (previous) stability window i.e. for $I_h = 105, 110, 120\ kA$. Only some of the most unstable eigenvalues are shown and for each of them the associated perturbation components are displayed together with the dominant contribution to the potential energy. The maximum value of the couplings involving (2,1) or (1,1) with any of the excited $(m_l, n_l)$ is also shown for comparison purposes. One sees that these couplings are insignificant i.e. $< 10^{-4}$ smaller than the dominant contribution. The particular case $I_h = 110\,kA$ and $\omega^2 = -5.832 \cdot 10^{-4}$ deserves some attention because the value of $W_p^{max\ (m,n)\times(m_l,n_l)}$ is large, i.e. $-2.20 \times 10^{-5}$, which is about 20 times smaller than $W_p^{max}$. The perturbation components involved in this coupling are $(1,1)$ and $(4,3)$; the $(2,1) \times (m_l, n_l)$ couplings continue to have a negligible role in determining the value of the potential energy. Among the leading contributions to the potential energy (those covering upto nearly one order of magnitude) none could be identified to result from the coupling between the (2,1) and non-resonant perturbation components. However, these last couplings are not insignificant and tend to give in general (very) weak destabilizing

contributions. Fig.5 illustrates another stability window obtained with the same plasma parameters as those from Fig.4 but with a larger value of the current in the TF coils i.e. $I_t = -180kA$. The larger toroidal field skews the magnetic field lines in the toroidal direction and in principle, the inverse rotational transform increases. The stability window corresponds to $115kA < I_h < 150\,kA$ and the $q$ profiles delimiting this interval can also be seen in Fig.5. A larger current in the HF coils is needed to reach the stability window and this occurs at an increased $q_{edge} \simeq 1.4$ (in the preceding case $q_{edge} \simeq 1.33$ see Fig.4).

# 5 Summary and conclusions

In this work we considered the global ideal MHD stability properties of free boundary plasmas with approximate helically symmetric cross-sections and nonzero toroidal plasma current. A simple $L = 2$ stellarator-like configuration of toroidal, helical and vertical field coils was proposed as a tool for studying the influence of the helical boundary shape (and through it of the external rotational transform) on the $(m, n) = (2, 1)$ external kink. An example of a complete set of plasma and coil parameters was given for the calculation of sequences of free boundary equilibria which approximately recovered the desired boundary shapes and such that the $q$ profiles were in the region of interest $1 < q < 2$. The parameter which was varied throughout the equilibrium sequence was the amount of current in the helical coils. These configurations are characterized by a spectrum of equilibrium Fourier components such that the couplings between the (2,1) perturbation component and the resonant $(m_l, n_l)$ perturbation components with $m_l > n_l > 1$ are negligible (in the fixed boundary calculations it was found that the $(m, n) \times (m_l, n_l)$ couplings with $m = n + 1$, $n = 1, 2, 3$ and $(m_l, n_l)$ as above, do not play any role in the determination of the global MHD stability with respect to external kinks). Finally, it has been shown that a helical (free) boundary deformation can stabilize the (2,1) external global mode at values of $q$ below 2.0 and $\beta$ values of the order of 1%. The stabilization occurs in a window of stability $I_h \in [I_h^{min}, I_h^{max}]$ where $I_h^{min}$ and $I_h^{max}$ depend on the equilibrium parameters. The fixed boundary results are thus generalized.

Before any comparison between these results and those of M.I.Mikhailov and V.D.Shafranov

c.f. Section I and Ref.[7] can be made, it is necessary to point out the important differences between the two studies: 1) In our case 3D geometries were considered. We have seen that, within the ideal MHD model, the couplings between (2,1) and the resonant components are insignificant but weak contributions due to the coupling with non resonant $(m_l, n_l)$, $n_l \neq 1$ may appear. 2) Our calculations were performed for $\beta > 0$. 3) The stability diagrams presented in Ref.[7] were derived under the assumption of a constant external rotational transform $\iota_h$ added artificially to the tokamak rotational transform; the $q$ profile was always monotonic. In the study presented here $\iota_h$ results directly from the currents in the HF coils and the total rotational is computed consistently with the equilibrium. The $q$ profiles are not necessarily monotonic and significant differences may exist between these profiles at the beginning and at the end of the equilibrium sequence. We add that our free boundary results are based only on calculations done for a $L = 2$ configuration with $N_{per} = 4$, an aspect ratio $\simeq 10$ and a couple of current density profiles. The whole set of available equilibrium parameters was not explored as was done in Ref.[8] and we cannot conclude on the possibility of stabilizing all ideal kink modes simultaneously. Such a problem was considered in Ref.[8] and we point out that the results were not so optimistic as those of Ref.[7].

# 6 Aknowledgements

This work was partly supported by EURATOM and the Swiss National Science Foundation. We thank Dr. S.P.Hirshman for providing us the VMEC code.

# References

[1] P.E.Moroz, Phys. Plasmas **3**, 3055 (1996)

[2] P.E.Moroz - Fusion Technology **30**, 40 (1996)

[3] P.E.Moroz, Plasma Phys. Control Fusion **39**, 1841 (1997)

[4] D.W.Ross,P.M.Valanju,H.He,W.H.Minner,P.E.Phillips,J.C.Wiley, A.J.Wootton,S.H.Zheng, Plasma Physics Reports, **23**, 492 (1996)

[5] K.Miyamoto, "Plasma Physics for Nuclear Fusion", MIT Press (1980)

[6] M.I.Mikhailov, V.D.Shafranov, Nuclear Fusion **30**, 413, (1990)

[7] M.I.Mikhailov, V.D.Shafranov, A.Subbotin, Proc. 22nd EPS Conf., Bournemouth, July 1995, Vol. 19C, Part III, p.193

[8] A.Ardelea, W.A.Cooper, Physics of Plasmas, **10**, 3482, (1997)

[9] S.P.Hirshman, U.Schwenn, J.Nührenberg, J. Comput. Phys. **87**, 396, (1990)

[10] D.V.Anderson, W.A.Cooper, R.Gruber, S.Merazzi, U.Schwenn, Int. J. Supercomp. Appl. **4**, 34 (1990)

[11] S.P.Hirshman, W.I.van Rij, P.Merkel, Comp. Phys. Communications, **43**, 143 (1986)

[12] W.A.Cooper, Plasma Physics and Controlled Fusion, **34**, No 6, 1011, (1992)

[13] R.Gruber, S.Semenzato, F.Troyon, T.Tsunematu, W.K.Kerner, P.Merkel, W.Schneider, Computer Physics Communications **24**, 363-376 (1981)

[14] A.H.Boozer - Phys. Fluids **23**, 904 (1980)

[15] W.A.Cooper,G.Y.Fu, in Proceedings of the joint Varenna-Lausanne international workshop, Varenna 1990, Theory of Fusion Plasmas, SIF Bologna (1990), 165

[16] C.Nuhrenberg, "Global ideal magnetohydrodynamic stability analysis for the configurational space of Wendelstein 7-X", Physics of Plasmas **3**, 2401 (1996)

Table 1 : *Some perturbation components with $m_l/n_l \leq 2$ resonant values and corresponding equilibrium coupling terms $(m_e, N_{per}n_e)$ ($(m_{e1}, n_{e1})$ or $(m_{e2}, n_{e2})$ depending on the $\pm$ sign in Eq.(5) for $(m,n) = (2,1)$ and $N_{per} = 4$. The equilibrium toroidal mode numbers correspond to one field period. A "-" symbol means that $n$, $n_l$ and the corresponding $n_{ei}$ cannot satisfy the periodicity requirements imposed by Eq.(5)*

Table 2 : *The 5 most unstable eigenvalues obtained when including the resonant $(m_l, n_l)$, $m_l > n_l > 1$ components in the study of the $(2,1)$ mode. The three values of $I_h$ belong to the stability window shown in Fig.4. The plasma parameters and coil configuration characteristics are given by Eq.(2) - see also Fig.1. The column to the right of $\omega^2$ identifies the perturbation components with the largest amplitudes. The quantity $W_p^{max}$ is the most important contribution to the potential energy and $W_p^{max\,(m,n)\times(m_l,n_l)}$ is the largest coupling between the (2,1) or (1,1) and any of the $(m_l, n_l)$ considered in the calculations.*

Figure 1 : *Stellarator-like configuration with 16 TF coils, two pairs of 2 HF coils and one pair of VF coils*

Figure 2 : *Free boundary equilibrium flux surfaces produced with VMEC. Each column represents the cross sections at one toroidal angle and each of the three rows are associated with one value of $I_h$. The coil system is represented in Figure 1. The parameters are those of Eq.(2). The three currents correspond to particular equilibria from the sequence shown in Fig.4 i.e. the first point and the two points just before and just after the stability window*

Figure 3.a : $\sqrt{g}_{m_e,n_e}$ *amplitudes for $s = 1$ (plasma boundary) for a fixed boundary equilibrium characterized by $L = 2$, $N_{per} = 4$, $1/\epsilon = 10$ (inverse aspect ratio), $\beta = 1\%$, with parabolic pressure profile. The x-axis corresponds to the $n_e$ equilibrium mode number. The points marked with '*' represent the equilibrium components responsible for couplings*

*between the* $(2,1)$ *mode and the* $(m_l, n_l)$ *perturbation components with* $m_l > n_l > 1$ *(only the* $n_e \leq 3$ *i.e.* $n_l \leq 13$ *are shown). All other equilibrium components are marked with 'o'. The fact that the* $\sqrt{g}_{m_e,n_e}$ *amplitudes with odd* $n_e$ *are extremely low is characteristic of the* $L = 2$ *fixed boundary configurations; only those* $\sqrt{g}_{m_e,n_e}$ *with* $n_e = 1,\ 3$ *are shown.*

Figure 3.b : $\sqrt{g}_{m_e,n_e}$ *amplitudes for the free boundary equilibrium described by Eq.(2). The x-axis corresponds to the* $n_e$ *equilibrium mode number. The '*' and 'o' symbols have the same meaning as in Fig 3.a but only the* $n_e \leq 2$ *i.e.* $n_l \leq 9$ *are shown. The* $\sqrt{g}_{m_e,n_e}$ *amplitudes with odd* $n_e$ *are larger than in the fixed boundary case but continue to remain very low compared to those with even* $n_e$

Figure 4 : *Study of the (2,1) mode:* **(a)** *toroidal plasma current density profile,* **(b)** $q(s)$ *profile,* **(c)** *sequence of most unstable eigenvalues* $\omega^2_{min}(I_h)$ *when the coil geometry and plasma parameters are given by Eq.(2). The aspect ratio is* $1/\epsilon \simeq 10$ *and the toroidal plasma current is* $J = 1.27 \cdot 10^5[A]$. *The inverse rotational transform profile is represented for* $I_h = 0.60 \times 10^5 A$ *(-),* $1.0 \times 10^5[A]$ *(- -) and* $I_h = 1.30 \times 10^5[A]$ *(·). The stability window is delimited by the two vertical lines and is associated with values of* $I_h$ *between* $1 \times 10^5[A]$ *and* $1.3 \times 10^5[A]$

Figure 5 : *The same as in Fig.4 but for* $I_t = -1.8 \times 10^5[A]$. *The inverse rotational transform profile is represented for* $I_h = 0.95 \times 10^5\,[A]$ *(-),* $1.15 \times 10^5[A]$ *(- -), and* $I_h = 1.50 \times 10^5[A]$ *(·) and the stability window corresponds to* $1.15 \times 10^5[A] < I_h < 1.50 \times 10^5[A]$

**Table 1** A.Ardelea

| $(m_l, n_l)$ | $(m_{e1}, n_{e1})$ | $(m_{e2}, n_{e2})$ | $(m_l, n_l)$ | $(m_{e1}, n_{e1})$ | $(m_{e2}, n_{e2})$ |
|---|---|---|---|---|---|
| ( 2 1 ) | ( 0 0 ) | - | ( 10 7 ) | - | ( 12 2 ) |
| ... | ... | ... | ( 11 7 ) | - | ( 13 2 ) |
| ( 4 3 ) | - | ( 6 1 ) | ... | ... | ... |
| ( 5 3 ) | - | ( 7 1 ) | ( 10 9 ) | ( 8 2 ) | - |
| ( 6 3 ) | - | ( 8 1 ) | ( 11 9 ) | ( 9 2 ) | - |
| ... | ... | ... | ( 12 9 ) | ( 10 2 ) | - |
| ( 6 5 ) | ( 4 1 ) | - | ( 13 9 ) | ( 11 2 ) | - |
| ( 7 5 ) | ( 5 1 ) | - | ... | ... | ... |
| ( 8 5 ) | ( 6 1 ) | - | ( 12 11 ) | - | ( 14 3 ) |
| ( 9 5 ) | ( 7 1 ) | - | ( 13 11 ) | - | ( 15 3 ) |
| ... | ... | ... | ( 14 11 ) | - | ( 16 3 ) |
| ( 8 7 ) | - | ( 10 2 ) | ( 15 11 ) | - | ( 17 3 ) |
| ( 9 7 ) | - | ( 11 2 ) | ... | ... | ... |

# **Table 2** A.Ardelea

| $I_h \cdot 10^5[A]$ | $q_{axis}$ | $q_{min}$ | $q_{edge}$ | $\omega^2$ | $(m_l, n_l)$ | | $W_p^{max}$ | $W_p^{max\ (m,n)\times(m_l,n_l)}$ |
|---|---|---|---|---|---|---|---|---|
| 1.050 | 1.437 | 1.273 | 1.273 | -9.889E-04 | 4 | 3 | -7.05E-04 | -4.81E-08 |
| | | | | -7.314E-04 | 9 | 7 | -6.80E-04 | -2.37E-11 |
| | | | | -2.073E-04 | 7 | 5 | -7.61E-04 | -4.22E-09 |
| | | | | -1.097E-04 | 4 | 3 | -3.45E-04 | -3.09E-09 |
| | | | | -9.354E-05 | 7 | 5 | -8.43E-04 | -6.85E-09 |
| 1.100 | 1.386 | 1.202 | 1.202 | -6.210E-04 | 11 | 9 | -3.58E-04 | -1.28E-08 |
| | | | | -5.832E-04 | 4 | 3 | -5.15E-04 | -2.20E-05 |
| | | | | -1.232E-04 | 4 | 3 | -6.89E-04 | -6.93E-07 |
| | | | | -9.435E-05 | 4 | 3 | -6.32E-04 | -4.09E-07 |
| | | | | -1.787E-05 | 4 | 3 | -4.17E-04 | -4.63E-07 |
| 1.200 | 1.286 | 1.065 | 1.065 | -3.104E-04 | 6 | 5 | -5.27E-04 | -3.20E-08 |
| | | | | -1.979E-04 | 8 | 7 | -2.20E-04 | 1.26E-09 |
| | | | | -1.877E-04 | 11 | 9 | -6.48E-04 | -5.41E-10 |
| | | | | -1.808E-04 | 6 | 5 | -5.03E-04 | -3.94E-08 |
| | | | | -1.145E-04 | 11 | 9 | -6.47E-04 | -1.99E-09 |

**Figure 1** A.Ardelea

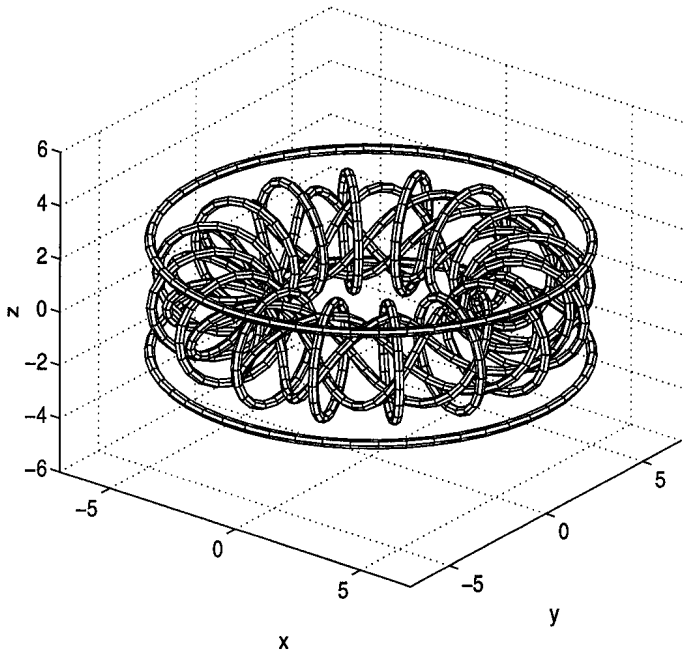

**Figure 2** A.Ardelea

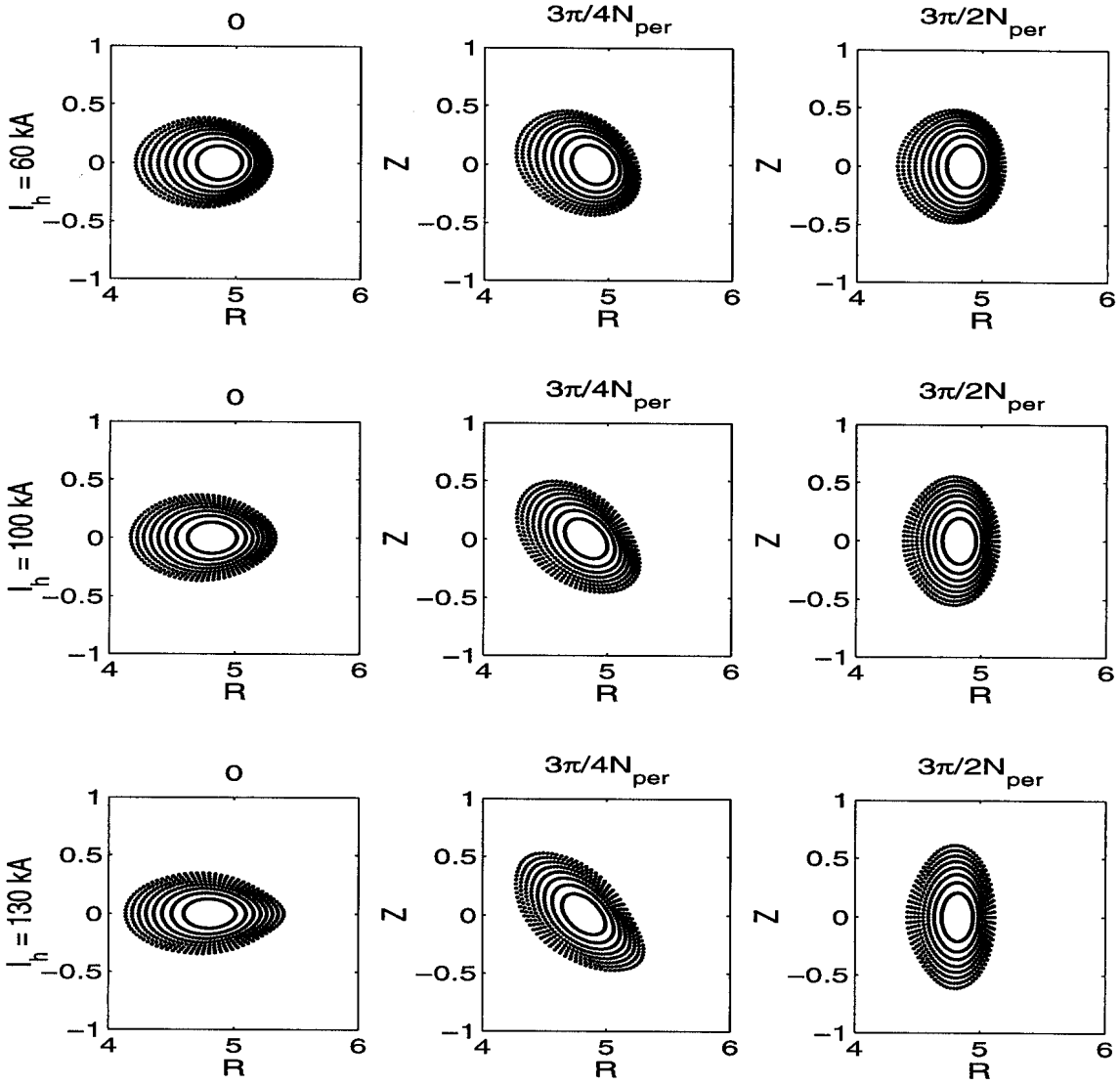

**Figure 3.a** A.Ardelea

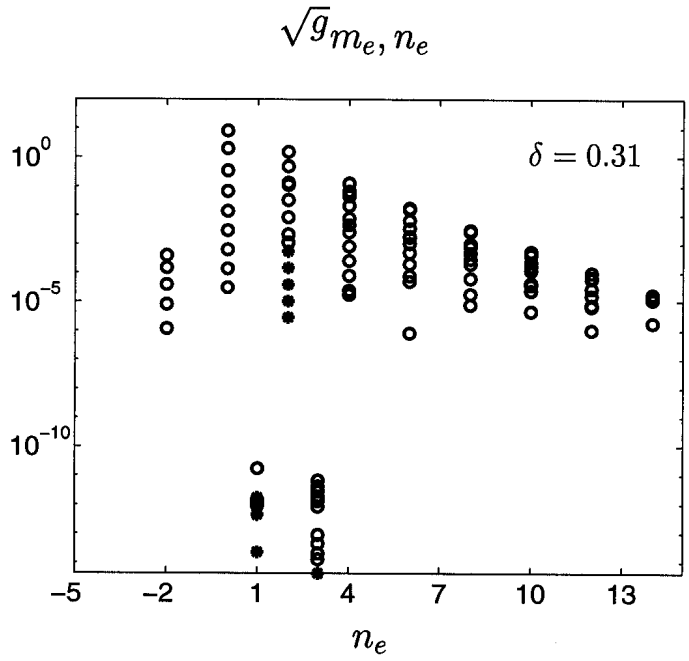

**Figure 3.b** A.Ardelea

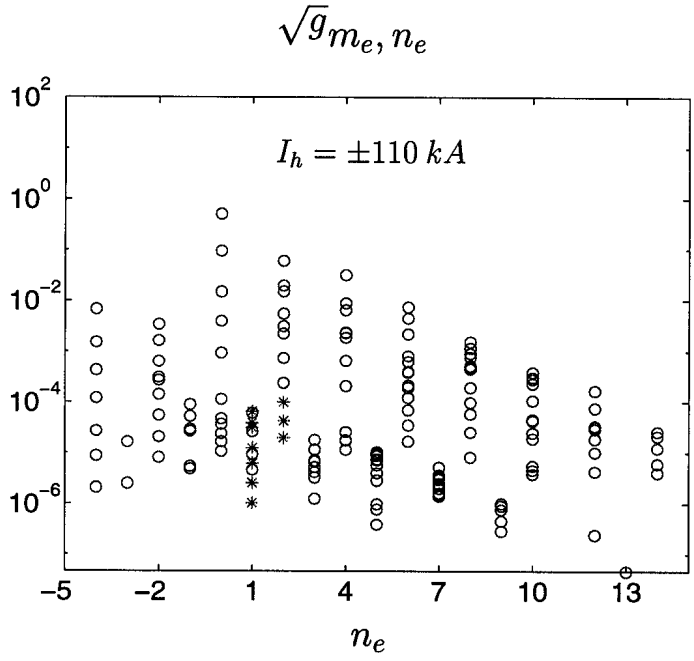

**Figure 4** A.Ardelea

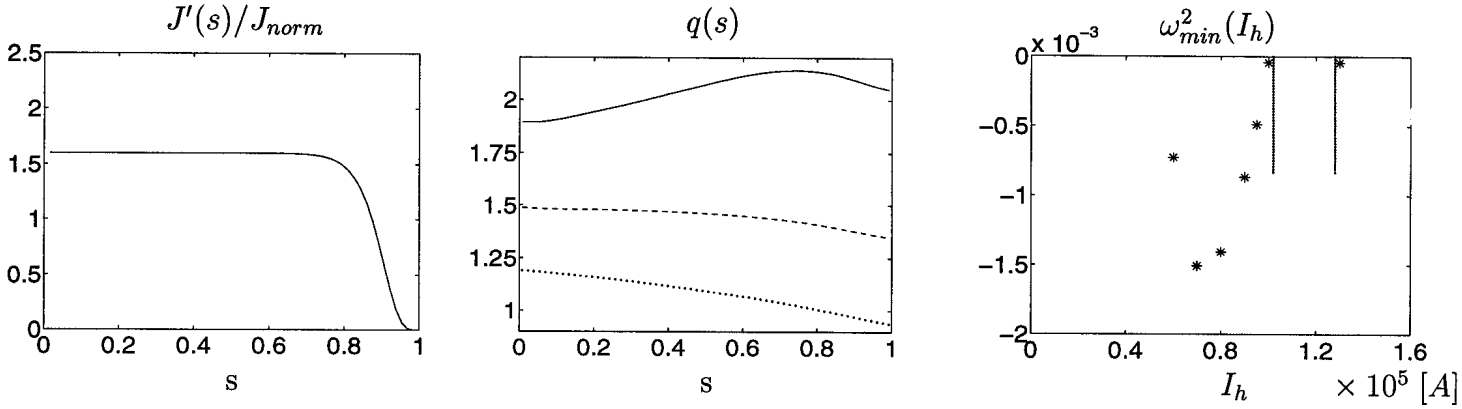

**Figure 5** A.Ardelea